



Universiteit
Leiden
The Netherlands

The electrode-electrolyte interface in CO₂ reduction and H₂ evolution: a multiscale approach

Cecilio de Oliveira Monteiro, M

Citation

Cecilio de Oliveira Monteiro, M. (2022, February 15). *The electrode-electrolyte interface in CO₂ reduction and H₂ evolution: a multiscale approach*. Retrieved from <https://hdl.handle.net/1887/3274033>

Version: Publisher's Version

License: [Licence agreement concerning inclusion of doctoral thesis in the Institutional Repository of the University of Leiden](#)

Downloaded from: <https://hdl.handle.net/1887/3274033>

Note: To cite this publication please use the final published version (if applicable).



10

Understanding cation trends for hydrogen evolution on platinum and gold electrodes in alkaline media

This chapter is based on Monteiro, M. C. O., Goyal, A., Moerland, P., Koper, M. T. M. *ACS Catalysis*, 11, 14328–14335 (2021)

Abstract

In this Chapter we study how the cation identity and concentration alter the kinetics of hydrogen evolution (HER) on platinum and gold electrodes. Previous work suggested an inverted activity trend as a function of alkali metal cation when comparing the performance of platinum and gold catalysts in alkaline media. We show that weakly hydrated cations (K^+) favor HER on gold only at low overpotentials (or lower alkalinity), whereas in more alkaline pH (or high overpotentials) the higher activity is found using electrolytes containing strongly hydrated cations (Li^+). We find a similar trend for platinum, however the inhibition of HER by weakly hydrated cations on platinum is observed already at lower alkalinity and lower cation concentrations, suggesting that platinum interacts stronger with metal cations than gold. We propose that weakly hydrated cations stabilize the transition state of the water dissociation step more favorably due to their higher near-surface concentration in comparison to a strongly hydrated cation such as Li^+ . However, at high pH and consequently higher cation concentrations, the accumulation of these species at the Outer Helmholtz Plane inhibits HER. This is especially pronounced on platinum, where a change in the rate determining step is observed at pH 13 when using a Li^+ or K^+ containing electrolyte.

10.1 Introduction

Efficient water electrolysis is an important technology towards a more sustainable society.¹ While water electrolysis in acidic media leads to the highest activity, it utilizes scarce and expensive materials (platinum, iridium); in alkaline media, more abundant materials can be used, but at the expense of a lower activity. To understand this difference in activity between the two media, the cathode reaction, i.e. hydrogen evolution (HER), has been studied extensively both in acidic and alkaline media. The focus of most works has been on tailoring the catalyst surface.^{2,3} However, metal cations in the electrolyte have been shown to have a significant effect on the activity of HER, although usually not taken into account in reaction mechanisms.^{4–7} In fact, the underlying mechanisms of the non-covalent interactions between cations and HER intermediates remain incompletely understood. Therefore, systematically studying electrolyte-related phenomena on different metal surfaces is desired, to improve our understanding of the underlying phenomena and to assist in further optimization of alkaline and proton exchange membrane (PEM) electrolyzers.

Platinum and gold are two model catalysts for understanding electrocatalytic reactions, including hydrogen evolution. Although two noble metals, it has been shown that the interaction of these surfaces with adsorbed species (reaction intermediates) and water is very different.^{8,9} Platinum is considered an optimal catalyst for HER (in acidic media), a consequence of the optimal hydrogen binding energy ($\Delta G_{\text{Hads}} \approx 0$). On the other hand, on gold electrodes, hydrogen binds weakly and the activity for HER at low overpotentials is significantly inferior to the activity found on Pt. Very recently, efforts have been dedicated to the effect that metal cations have on the activity of HER on different metal surfaces. A main contribution has been made by Xue et al.⁷ who studied the HER activity of Pt, Ir, Au, and Ag in alkaline media, as a function of the cation identity (Li^+ , Na^+ , K^+ , Rb^+ , Cs^+). They report that weakly hydrated cations such as Cs^+ favour HER on Au and Ag while they are detrimental to the reaction activity on Pt and Ir. The authors explain this "inverted" trend based on the binding energy of hydrogen to the metal, which weakens as a function of the alkali metal cation: $\text{Cs}^+ > \text{Rb}^+ > \text{K}^+ > \text{Na}^+ > \text{Li}^+$. They propose that weakly hydrated cations as Cs^+ are beneficial to HER on Au and Ag electrodes, which lie on the weak binding side of the activity volcano, while being detrimental to HER on Pt and Ir, due to an over stabilization of the adsorbed intermediates.

The hydrogen adsorption energy is generally considered to be an accurate descriptor for HER activity in acidic media, where the adsorbed hydrogen is formed from proton/hydronium (H_3O^+) reduction. However, in alkaline media, where water dissociation has to occur in order for hydrogen to adsorb, other descriptors appear to be needed to describe activity trends.⁸ On platinum, the hydrogen binding energy (HBE) is derived from the underpotential hydrogen region (H_{upd}) in the blank voltammetry.^{10,11} A positive shift of the H_{upd} peak, for example as a function of pH, has been ascribed to an increase in the hydrogen binding energy and an associated lower activity for HER. However, it has been shown that this positive shift is actually associated with a weakening of the OH adsorption on Pt {100} and {110} steps and facets due to the presence of alkali metal cations at the reaction interface.¹² The so-called H_{upd} region is therefore a hydrogen-cation-hydroxyl region, and therefore it cannot serve as a simple activity descriptor. The nature of the rate-determining step for HER in alkaline media is still under debate. The work of Markovic et al. suggests that on platinum, in alkaline media, water dissociation is the rate determining step.⁵ However, Liu et al.⁴ suggests that for a similar system, the driving force for OH desorption weakens in the order $\text{Li}^+ > \text{Na}^+ > \text{K}^+$, and this trend gives rise to the HER activity trend of $\text{LiOH} > \text{NaOH} > \text{KOH}$ at pH 13. Gold is a much less investigated catalyst for HER, but of interest as a catalyst for the electrocatalytic reduction of carbon dioxide, for which HER is a competing reaction.¹³ As discussed above, an inverted activity trend ($\text{K}^+ > \text{Na}^+ > \text{Li}^+$), compared to platinum, has been reported for gold electrodes in 0.1 M MOH.⁷ Our recent work on polycrystalline gold and Au(111) in alkaline media (NaOH), shows that up to pH 11, increasing the Na^+ concentration significantly enhances the HER activity.¹⁴ At higher pH (>12) and consequently high (near-surface) cation concentrations, the activity for HER decreases, likely due to a blockage effect. However, this phenomenon has not yet been investigated for other metal surfaces, as a function of the cation identity.

Taking the hydrogen binding energy as a descriptor, cannot explain the different cation trends for HER on Pt and Au as a function of the cation identity. This is especially relevant in alkaline media, where our recent work has shown that the local pH and cation concentration are two interrelated variables.^{13–15} Therefore, in this Chapter, we have systematically investigated the effect of pH and cation concentration on the activity for HER on polycrystalline Pt and Au, comparing electrolytes containing weakly (K^+) and strongly (Li^+) hydrated cations. In alkaline media, on gold, we see that the surface blockage phenomena (previously observed at pH 13 in Na^+ containing electrolyte) is not present in a Li^+ containing electrolyte,

due to the less pronounced accumulation of Li^+ ions near the surface, even at high pH. In contrast, K^+ ions are detrimental to the reaction activity above pH 13. Similar behavior is observed on platinum, however already at pH 11, and at low cation concentrations, suggesting that cations interact stronger with Pt than with Au electrodes. These results show that on Pt in alkaline media, cations typically act as inhibitors, whereas on gold in alkaline media, cations can act as either a promotor or an inhibitor, depending on their local accumulation in the double layer.

10.2 Hydrogen evolution in alkaline media

We initially studied how cations affect the hydrogen evolution reaction (HER) on polycrystalline platinum and gold electrodes using stationary cyclic voltammetry, and the results are shown in Fig. 10.1a-c. We carried out the experiments in alkaline media (pH 13) and we find that K^+ cations promote water reduction on gold, while they are detrimental to the reaction on platinum, in agreement with the results found by Xue et al. for Au(111) and polycrystalline Pt at the same pH and similar overpotentials.⁷ We have also recorded the blank voltammetry of the polycrystalline platinum electrode in alkaline media and a positive shift of the H_{upd} peak in K^+ containing electrolyte is also found at pH 13 (Fig. 10.1c). Similar measurements were performed in acidic media (see Fig. G.1a-c and discussion in Appendix G). There, water reduction is promoted by weakly hydrated cations on both gold and platinum, and a similar (but less pronounced) positive shift in the H_{upd} of the platinum electrode is found in K^+ electrolyte. Although the effect of the different cations on water reduction on platinum is inverted for acidic and alkaline media, it seems that at both pH weakly hydrated cations interact with the adsorbed H/OH in a similar fashion, suggesting that the mechanism behind this inverted trend goes beyond just an effect on the hydrogen binding energy, as proposed by Xue et al.⁷ A more pronounced positive shift in the H_{upd} at pH 13, in comparison to pH 3 was also observed by Chen et al.¹² In the same work, DFT calculations suggest that higher coverages of alkali metal cation adsorbed along the steps of Pt(553) becomes more favourable by increasing electrolyte pH (at the same potential on an RHE scale). Therefore, we expect that the larger shift we observe on polycrystalline platinum for the experiment carried out at pH 13 is due to an increase in the cation- OH_{ads} - H_{ads} interactions, at higher cation coverages. The blank voltammetry of the polycrystalline gold and platinum electrode, taken before the measurements shown in , can be seen in Fig. G.2 in Appendix G.

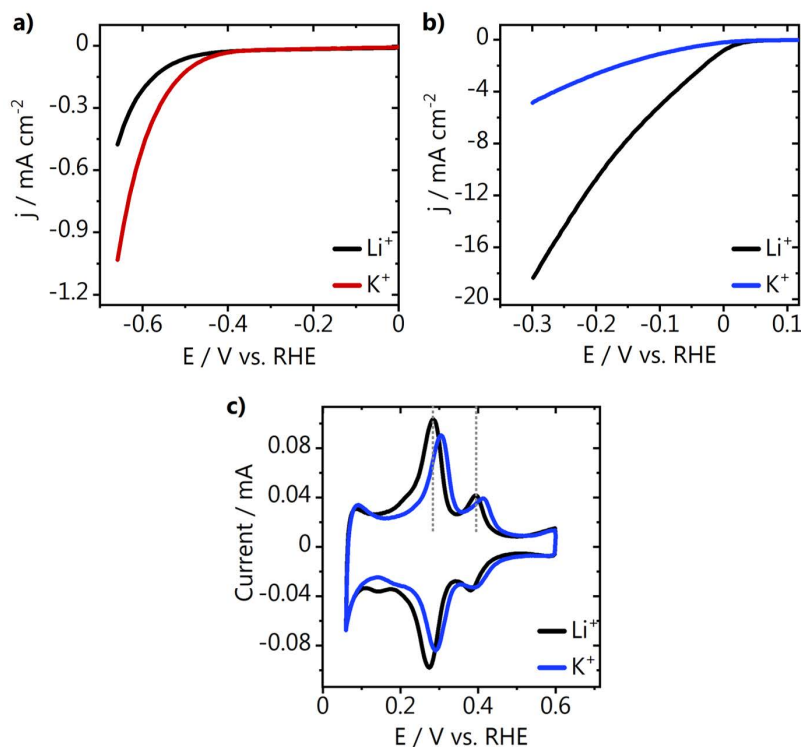


Fig. 10.1. Stationary hydrogen evolution on **a)** gold and **b)** platinum in alkaline media (0.1 M MOH, pH = 13), together with **c)** the blank voltammetry of the platinum electrode. $M = \text{Li}^+$ or K^+ . The voltammetry was recorded at 50 mV s^{-1} .

In Fig. 10.2 we show the Tafel slopes, derived from the cyclic voltammograms from Fig. 10.1 and Fig. G.1 (Appendix G), as a function of the applied potential. Eq. 10.1-10.5 display the three accepted reaction steps during proton (H_3O^+) or water reduction, with the rate-determining step in the mechanism that can be derived from Tafel slope analysis in parenthesis.¹⁶ Here * represent a free surface adsorption site. Tafel slopes of around 120 mV dec^{-1} are obtained for the gold electrode in the Li^+ and K^+ electrolytes, in both acidic and alkaline media. This indicates that at the potentials studied, in both cases the activity for HER is controlled by the first electron transfer step (Volmer step, Eq. 10.1), which in alkaline media is in fact governed by the barrier of the electrochemical water dissociation (Eq. 10.2). The latter is in agreement with our previous studies in Na^+ containing electrolyte.¹⁴ For platinum, in acidic media, Tafel slopes of around 40 mV dec^{-1} imply that the second electron transfer Heyrovsky step (Eq. 10.3) is the rate determining step, in both Li^+ and K^+ electrolyte.¹⁷ In contrast, in alkaline media, where we see higher HER activity

in Li^+ than K^+ , the Tafel slopes indicate that in Li^+ the Heyrovsky step is still rate determining while there seems to be a change in the reaction mechanism in K^+ electrolyte. A Tafel slope of 112 mV dec^{-1} suggests either the Volmer step or a Heyrovsky step at high coverage of adsorbed hydrogen (at high overpotentials) as the rate limiting step. Considering the Tafel analysis was performed using the current response at low overpotentials, the Volmer step is more likely to be the rate determining step here. This change in the reaction mechanism on platinum suggests that the cation identity plays an important role on how accessible the surface is for hydrogen adsorption.

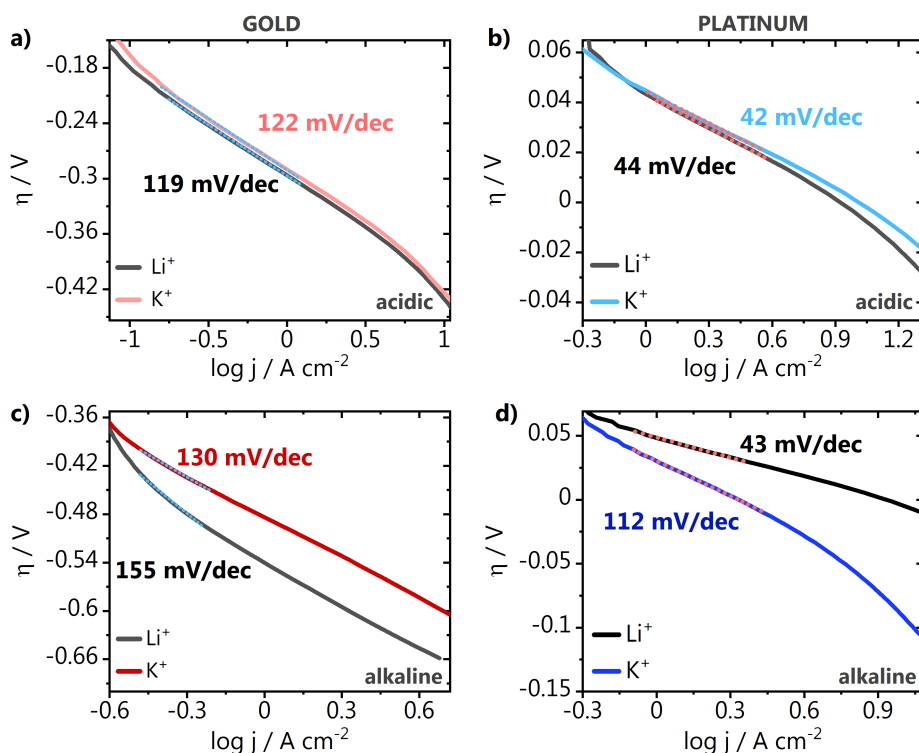
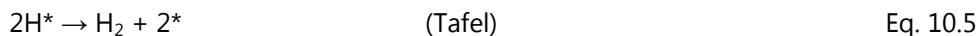


Fig. 10.2. Tafel slopes derived from the stationary cyclic voltammetry, recorded on **a)** gold and **b)** platinum in acidic media (0.1 M M_2SO_4 , pH = 3), as well as for **c)** gold **d)** platinum in alkaline media (0.1 M MOH , pH = 13). $M = \text{Li}^+$ or K^+ . The range used for the curve fitting is indicated in all plots with a dotted line.



Previous work reported higher HER activity for gold in electrolytes containing weakly hydrated cations, in the order $\text{Cs}^+ > \text{K}^+ > \text{Na}^+ > \text{Li}^+$, and the opposite trend was observed for platinum electrodes in alkaline media.⁷ However, experiments on gold have usually been carried out in a limited potential range, as at large overpotentials currents become impractical, i.e. due to bubble formation and a consequent loss of potential control. To further elucidate the nature of this "inverted" trend, we have performed HER on gold at pH 11 and 13 over a wide potential range in electrolytes containing Li^+ , Na^+ and K^+ cations (Fig. 10.3). As shown in Fig. 10.3a, at pH 13 and low overpotentials, indeed the activity trend is found to be $\text{K}^+ > \text{Na}^+ > \text{Li}^+$. Remarkably, at more negative overpotentials (-0.8 V vs. RHE) the trend inverts, and a higher current is obtained in the Li^+ electrolyte. This strongly suggests that on gold, upon an increase in the local alkalinity at high overpotentials, and consequent increase in the near-surface cation concentration, weakly hydrated cations are actually detrimental to water reduction. This is likely due to an accumulation at the reaction interface and blockage of the surface, as proposed in our previous work.¹⁴ This blockage effect is less pronounced in Na^+ and even less in the Li^+ electrolyte, as the stronger binding of water molecules in the hydration shell of these cations prohibit their accumulation at the Outer Helmholtz Plane (OHP), as we have also shown in Chapter 8 through DFT based *Ab Initio* Molecular Dynamics (AIMD) simulations on the interaction of alkali cations with Au(111).¹⁸

To further support these observations, we have performed the same experiment at pH 11, where there is in principle a lower driving force for cations to accumulate near the surface than at pH 13, due to the lower interfacial electric field strength. As shown in Fig. 10.3b, at pH 11 the inversion of the HER activity trend as a function of the cation identity happens at ca. 0.25 V more negative potential than at pH 13. This confirms that the local alkalinity defines the concentration of cations near the surface, and that weakly hydrated cations hinder HER on gold if their local concentration is high enough. This behaviour is similar to platinum, although on

platinum this effect is already observed at lower overpotentials, whereas on gold more driving force is required. At pH 11, more current is required to reach high local alkalinity, while at pH 13 this happens at lower overpotentials.

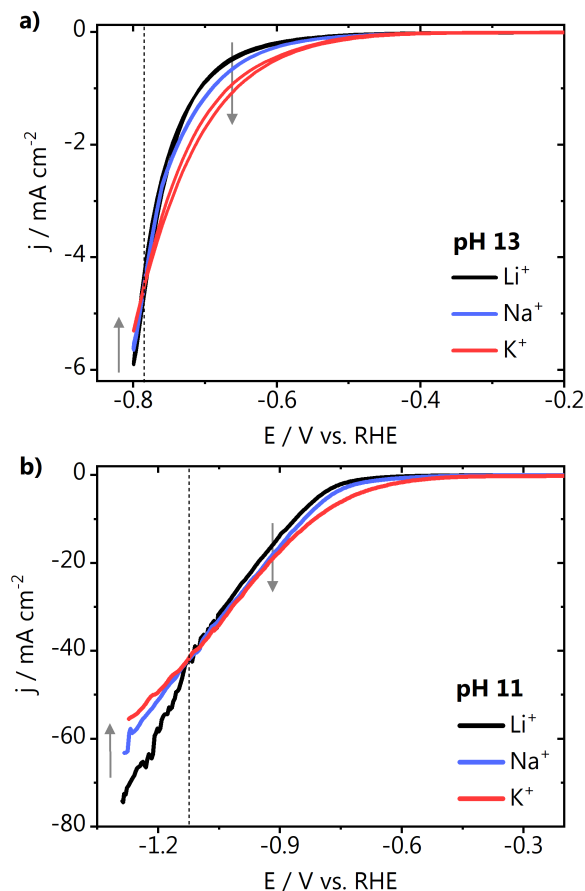


Fig. 10.3. Stationary hydrogen evolution cyclic voltammetry on gold at pH **a)** 13 and **b)** 11 recorded in 0.1 M MOH and 0.001 M MOH, with $M = \text{Li}^+, \text{Na}^+ \text{ or } \text{K}^+$ at 50 mV s^{-1} . The dotted gray lines indicate the potential in which the CVs cross and the arrows point going from the strongly to the weakly hydrated metal cation species.

10.3 Cation concentration dependence

The results shown in Fig. 10.3a and Fig. 10.3b suggest that the cation trends for HER on platinum and gold are not actually "inverted" as previously stated⁷, but just depend on the reaction conditions, such as bulk/local pH, near-surface cation concentration and cation identity. In order to further elucidate that, we have performed HER under well-defined mass transport conditions, using rotating disc electrodes (RDE) of gold and platinum. We changed the cation concentration in electrolytes having different bulk pH, and observed the effect of those variables on the HER kinetics. The HER cyclic voltammetry on gold is shown in Fig. G.4 in Appendix G, and the correspondent reaction order plots in Fig. 10.4. In the Li^+ containing electrolyte, a positive reaction order is found both at pH 11 and 13, differently from what we observed for instance for Na^+ in our previous work.¹⁴ In the case of K^+ , at pH 11 a higher cation concentration promotes HER, as shown by the higher reaction order than found in Li^+ . However, at pH 13 we see a negative reaction order, with HER being inhibited as the concentration of K^+ increases.

The HER inhibition in alkaline pH seems to be more pronounced for weakly hydrated cations and need less driving force to be observed on platinum than on gold, as we show in Fig. 10.1. To better define the experimental conditions in which this phenomenon takes place, we performed similar experiments as shown in Fig. 10.4 on platinum, also using a rotating disc electrode. The cyclic voltammetry is shown in Fig. G.5 (Appendix G) and the correspondent reaction order plots are depicted in Fig. 10.5. It is important to point out that although the electrolytes in this work were used as received, no metal contaminants are expected to affect our measurements, as evidenced by the overlapping consecutive CVs shown in Fig. G.6 in Appendix G.¹⁹ We see in Fig. 10.5a and Fig. 10.5b that, similarly to gold, on platinum, increasing the concentration of Li^+ cations promotes HER both at pH 11 and 13. In contrast, for the K^+ electrolyte, at pH 9 and 10 we observe at low K^+ concentration a positive reaction order, and that at the highest concentrations HER starts to be inhibited, confirming the relationship between local alkalinity and concentration of weakly hydrated cations at the reaction interface. At pH 11, while on gold we see a promotion of HER by increasing the K^+ concentration, for platinum we observe a negative reaction order, with even more negative values at pH 12. This indicates that weakly hydrated metal cations in the electrolyte interact stronger with platinum than with gold electrodes, under the same experimental conditions.

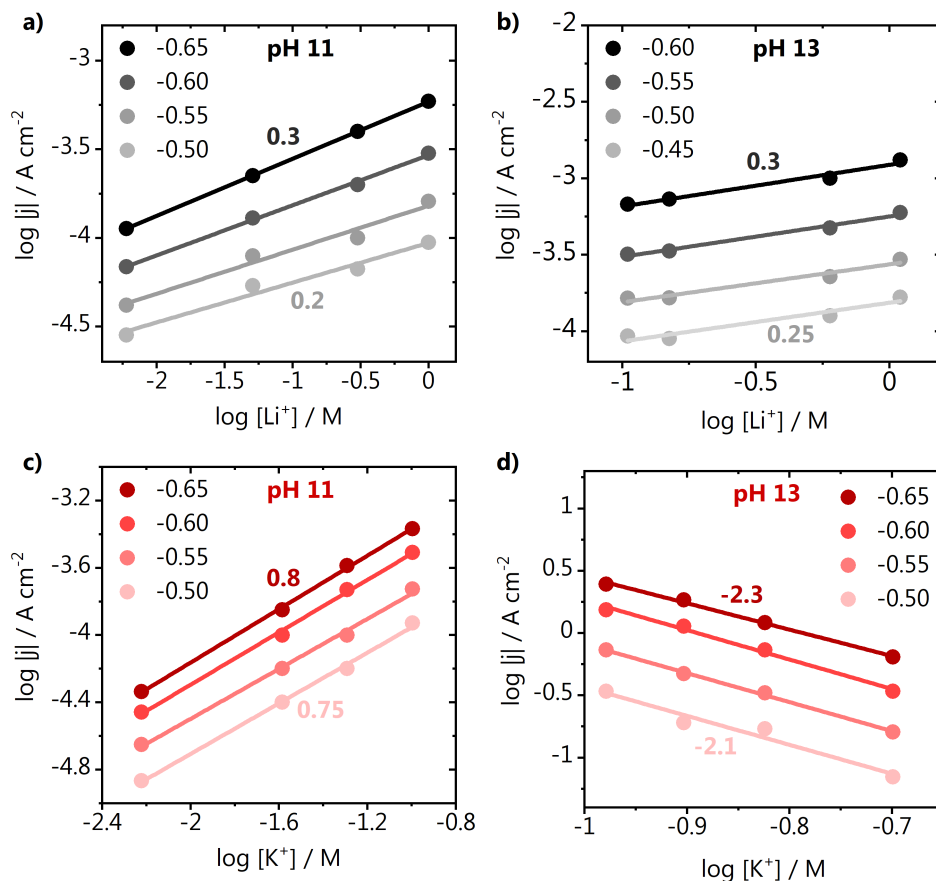


Fig. 10.4. Reaction order plot of HER on polycrystalline gold in the cation concentration at pH 11 and 13 in **a)-b)** Li^+ and **c)-d)** K^+ containing electrolyte. The current is reported for 50 mV potential steps (vs. RHE) plotted as a function of the logarithm of the current density on the y-axis and logarithm of the cation concentration on the x-axis. The slopes extracted from the linear fit of the current response (reaction orders) are shown next to the plots. The slope at the top corresponds to the most negative potential applied and the slope at the bottom to the most positive, as indicated also by the colors. CVs are shown in Fig. G4 and were recorded using a rotating disc electrode, at 25 mV s^{-1} and 2500 rpm.

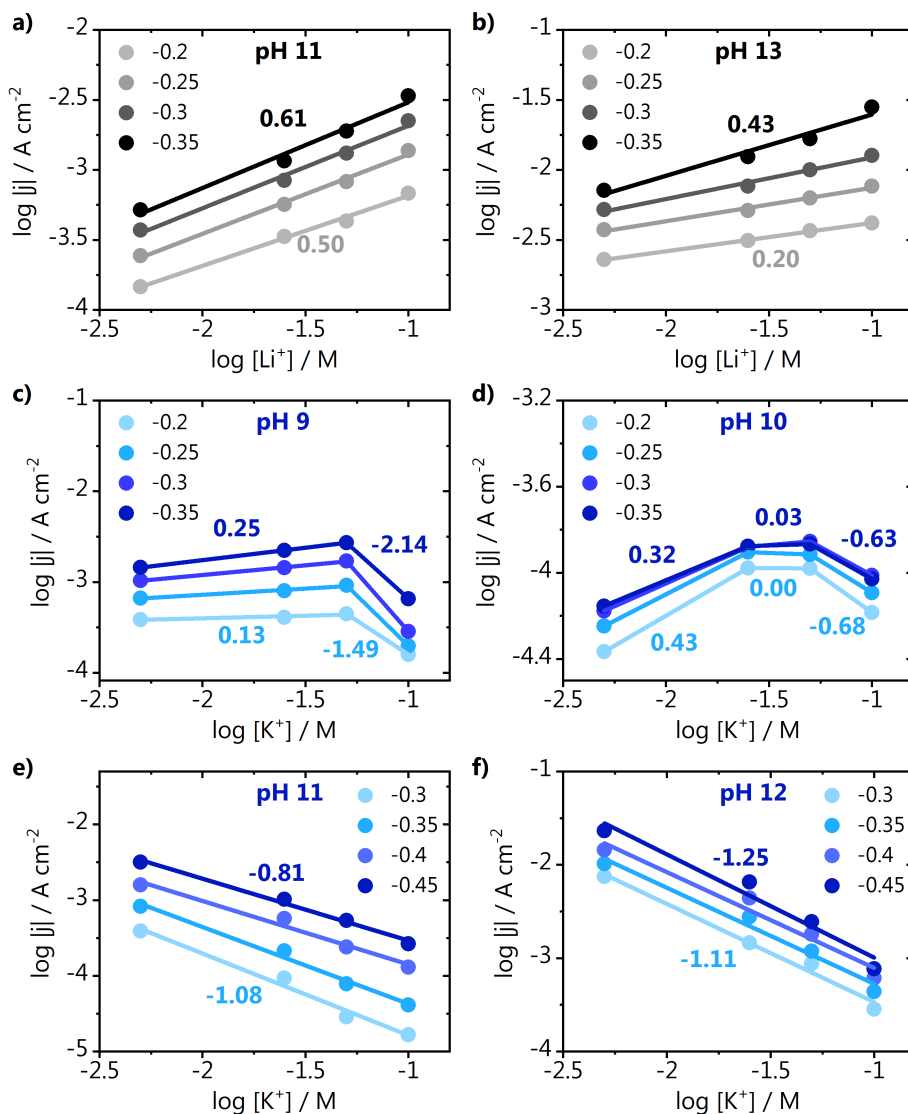


Fig. 10.5. Reaction order plot of HER on polycrystalline platinum in the cation concentration at pH 11 and 13 in **a)-b)** Li^+ and pH 9-12 in **c)-d)** K^+ containing electrolyte. The current is reported for 50 mV potential steps (vs. RHE) plotted as a function of the logarithm of the current density on the y-axis and logarithm of the cation concentration on the x-axis. The slopes extracted from the linear fit of the current response (reaction orders) are shown next to the plots. The slope at the top corresponds to the most negative potential applied and the slope at the bottom to the most positive, as indicated also by the colors. CVs are shown in Fig. G5 and were recorded using a rotating disc electrode, at 25 mV s^{-1} and 2500 rpm.

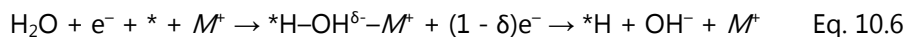
10.4 Discussion

The opposite cation trends for HER on platinum and gold electrodes in alkaline media have previously been explained using the hydrogen binding energy as a descriptor for HER.²⁰ However, our recent work has shown that although this might be a suitable descriptor for HER in acidic media, on gold, in alkaline media, the rate of this reaction depends on the near-surface pH and near-surface cation concentration.¹⁴ In our present work we elucidate that the inverted cation trend between platinum and gold strongly depends on the cation identity, the electrolyte bulk pH and the local alkalinity. We see that on gold, HER is promoted by weakly hydrated cations only at low current densities and moderately alkaline pH, as shown in Fig. 10.3. This is confirmed by the different cation reaction orders on polycrystalline Pt and Au as a function of pH, potential, and cation identity. For gold, we find a positive reaction order in a Li^+ electrolyte at pH 13, while in K^+ electrolyte there is an inhibition of HER at the same pH. The same is observed for platinum, however on this electrode HER starts to be inhibited already at lower pH and lower cation concentrations, indicating that metal cations interact stronger with platinum than with gold electrodes. Additionally, on platinum we see a change in the reaction mechanism as a function of the electrolyte cation: in Li^+ electrolyte the Heyrovsky step is the rate determining step and in K^+ the Volmer step seems to be rate determining. These differences of cation interaction with gold and platinum have also been suggested by other studies. For instance, DFT calculations presented in the work of Hersbach et al.²¹ indicate that cation adsorption is more energetically favourable on platinum {111} and {100} facets than on gold. Additionally, work from our group has reported an anomalously large diffuse-layer Gouy-Chapman capacitance for the Pt(111)-aqueous electrolyte interface in comparison to Au(111) and Hg.²² It shows that the double layer of Pt(111) (and to some extent also of Au(111)) is more compact than predicted by Gouy-Chapman theory, because the electrolyte interacts stronger with Pt than with Au and Hg. Therefore, we suggest that at the cathodic potentials in which HER takes place, the driving force for cations to accumulate near the platinum surface is higher.

Site blocking by metal cations has been previously proposed in various works. An early report by Herasymenko and Šlendyk assumed a simple competitive Langmuir adsorption model to rationalize cation trends for HER, which was later further rationalized in the work of Frumkin considering the effect of cation adsorption on reaction rates.^{23,24} The specific adsorption of cations on catalytic sites

for HER has been extensively discussed in the recent review of Waegle et al.²⁵, showing that despite various theoretical and experimental evidences, it is still unclear under which specific conditions (potential, pH, concentration, electrode surface) cations specifically adsorb, if they do at all. Another site-blocking theory has been put forward by Markovic and co-workers, in which they propose that non-covalent interactions between hydrated alkali metal cations $M^+(H_2O)_x$ and adsorbed OH (OH_{ad}) give rise to $OH_{ad}-M^+(H_2O)_x$ clusters at the interface. They propose the concentration of these clusters increases in the same order as the hydration energies of the corresponding cations ($Li^+ \gg Na^+ > K^+ > Cs^+$). However, we can rule out this being the reason for the inhibition of HER that we observe in our experiments, as we find positive reaction orders in Li^+ electrolyte both on gold and platinum (see Fig. 10.4 and Fig. 10.5), and the inhibition effect is only seen in K^+ electrolyte (and in our previous work in Na^+).¹⁴

Based on our results and the work discussed above, we propose that the model that we recently formulated for cation effects in HER on gold in alkaline media, is more broadly applicable. That model has two regimes, depending on local cation concentration: a promotion regime, and an inhibition regime (see Fig. 10.6). In the promotion regime (low cation concentration, low pH), both strongly and weakly hydrated cations stabilize the transition state of the first electron transfer step, the water dissociation (Eq. 10.6).¹⁴



Weakly hydrated cations lead then to higher activity due to their stronger driving force to accumulate at the OHP and consequently higher concentration at the interface, as we have shown in Chapters 8 and 9 both through experiments and simulations.¹⁸ We see that this promotion regime is more limited for platinum than for gold, due to stronger interaction of metal cations with platinum, already pronounced in weakly alkaline conditions and moderate cation concentrations. In case of such a very strong interaction, the promotion regime develops into the inhibition regime, in weakly hydrated cations accumulate near the surface to such an extent that they hinder the access of water to the reaction interface or lower the availability of free surface sites. In this regime, the HER has a negative reaction order on cation concentration. Experiments with Pt electrodes are typically in this inhibition regime, whereas experiments with Au are typically in the promotion

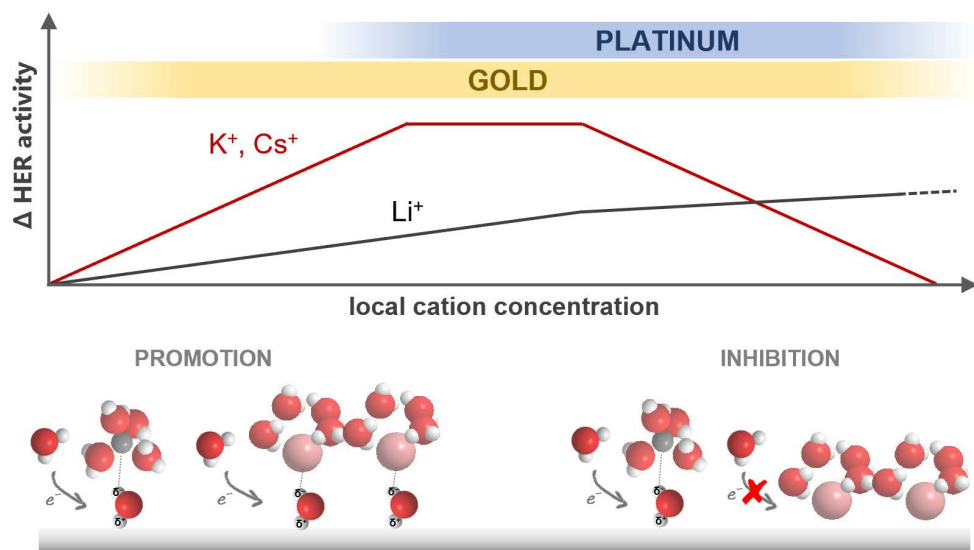


Fig. 10.6. Schematic representation of the effect of cation concentration on the activity of HER comparing platinum and gold, together with a pictorial description of the mechanism through which weakly (K^+ , Cs^+) and strongly (Li^+) hydrated cations promote and/or inhibit HER.

regime. This model explains the inverted cation dependence between Pt and Au, observed here as well as in previous work.²⁰

Our findings may have important implications for electrolyzers in which HER is the cathode reaction. Due to the high current densities of operation, a high local alkalinity can develop near the cathode surface. As our work shows, depending on the electrolyte cation identity, the activity for HER can be compromised upon local alkalization of the reaction interface. Tuning the cathode geometry and consequently enhancing the transport of species, or selecting a specific cation, can help to mitigate these negative effects.

10.5 Conclusions

In this work we have elucidated the cation effects on HER on gold and platinum electrodes in alkaline media. Through cyclic voltammetry and rotating disc electrode experiments we investigated HER in alkaline media in electrolytes containing strongly and weakly hydrated cations, namely Li^+ , Na^+ , and K^+ . In agreement with the model that we recently formulated for HER on gold, we show here that for platinum there are also two distinct regimes for how cations affect

HER, according to the cation concentration. At low cation concentration and mildly alkaline media, both weakly and strongly hydrated cations promote HER on gold and platinum. At more alkaline pH and consequently higher near-surface cation concentrations, HER is inhibited by weakly hydrated cations. This inhibition regime is observed for platinum at lower alkalinity and cation concentration than for gold electrodes, as platinum interacts stronger with cations in the electrolyte. On platinum, based on Tafel slopes, we find a change in the reaction mechanism at pH 13 from the Heyrovsky to the Volmer step, when the reaction is carried out in Li^+ or K^+ electrolyte, respectively. This can be understood as an inhibition of the Volmer step in K^+ electrolyte, whereas Li^+ actually promotes the Volmer step. The observation that HER on gold is mostly in the promotion regime, whereas HER on platinum is mostly in the inhibition regime, explains the previously observed inverted cation dependence of HER on gold and platinum. Our work shows the complexity of the electrode-electrolyte interface during hydrogen evolution on platinum and gold, and that to achieve high activity, cation identity and near-surface cation concentration are crucial activity descriptors, with the latter depending on the electrolyte pH and metal surface employed.

References

- (1) Shiva Kumar, S.; Himabindu, V. *Mater. Sci. Energy Technol.* 2019, *2* (3), 442–454.
- (2) Strmcnik, D.; Lopes, P. P.; Genorio, B.; Stamenkovic, V. R.; Markovic, N. M. *Nano Energy* 2016, *29*, 29–36.
- (3) Zhou, Z.; Pei, Z.; Wei, L.; Zhao, S.; Jian, X.; Chen, Y. *Energy Environ. Sci.* 2020, *13* (10), 3185–3206.
- (4) Liu, E.; Li, J.; Jiao, L.; Doan, H. T. T.; Liu, Z.; Zhao, Z.; Huang, Y.; Abraham, K. M.; Mukerjee, S.; Jia, Q. *J. Am. Chem. Soc.* 2019, *141* (7), 3232–3239.
- (5) Subbaraman, R.; Tripkovic, D.; Chang, K.-C.; Strmcnik, D.; Paulikas, A. P.; Hirunsit, P.; Chan, M.; Greeley, J.; Stamenkovic, V.; Markovic, N. M. *Nat. Mater.* 2012, *11* (6), 550–557.
- (6) Huang, B.; Muy, S.; Feng, S.; Katayama, Y.; Lu, Y. C.; Chen, G.; Shao-Horn, Y. *Phys. Chem. Chem. Phys.* 2018, *20* (23), 15680–15686.
- (7) Xue, S.; Garlyyev, B.; Watzele, S.; Liang, Y.; Fichtner, J.; Pohl, M. D.; Bandarenka, A. S. *ChemElectroChem* 2018, *5* (17), 2326–2329.
- (8) Dubouis, N.; Grimaud, A. *Chem. Sci.* 2019, *10* (40), 9165–9181.
- (9) Huang, B.; Myint, K. H.; Wang, Y.; Zhang, Y.; Rao, R. R.; Sun, J.; Muy, S.; Katayama, Y.; Corchado Garcia, J.; Fraggedakis, D.; Grossman, J. C.; Bazant, M. Z.; Xu, K.; Willard, A. P.; Shao-Horn, Y. *J. Phys. Chem. C* 2021, *125* (8), 4397–4411.
- (10) Jiao, L.; Liu, E.; Mukerjee, S.; Jia, Q. *ACS Catal.* 2020, *10* (19), 11099–11109.
- (11) Weber, D. J.; Janssen, M.; Oezaslan, M. *J. Electrochem. Soc.* 2019, *166* (2), F66–F73.
- (12) Chen, X.; McCrum, I. T.; Schwarz, K. A.; Janik, M. J.; Koper, M. T. M. *Angew. Chemie - Int. Ed.* 2017, *56* (47), 15025–15029.
- (13) Goyal, A.; Marcandalli, G.; Mints, V. A.; Koper, M. T. M. *J. Am. Chem. Soc.* 2020, *142* (9), 4154–4161.
- (14) Goyal, A.; Koper, M. T. M. *Angew. Chemie Int. Ed.* 2021, *60* (24), 13452–13462.
- (15) Goyal, A.; Koper, M. T. M. *J. Chem. Phys.* 2021, *155* (13), 134705.
- (16) Shinagawa, T.; Garcia-Esparza, A. T.; Takanabe, K. *Sci. Rep.* 2015, *5* (1), 13801.
- (17) Ledezma-Yanez, I.; Wallace, W. D. Z.; Sebastián-Pascual, P.; Climent, V.; Feliu, J. M.; Koper, M. T. M. *Nat. Energy* 2017, *2* (4), 1–7.
- (18) Monteiro, M. C. O.; Dattila, F.; Hagedoorn, B.; García-Muelas, R.; López, N.; Koper, M. T. M. *Nat. Catal.* 2021, *4* (8), 654–662.
- (19) Li, X.; Gunathunge, C. M.; Agrawal, N.; Montalvo-Castro, H.; Jin, J.; Janik, M. J.; Waagele, M. M. *J. Electrochem. Soc.* 2020, *167* (10), 106505.
- (20) Xue, S.; Garlyyev, B.; Watzele, S.; Liang, Y.; Fichtner, J.; Pohl, M. D.; Bandarenka, A. S. *ChemElectroChem* 2018, *5* (17), 2326–2329.
- (21) Hersbach, T. J. P.; McCrum, I. T.; Anastasiadou, D.; Wever, R.; Calle-Vallejo, F.; Koper, M. T. M. *ACS Appl. Mater. Interfaces* 2018, *10* (45), 39363–39379.
- (22) Ojha, K.; Arulmozhi, N.; Aranzales, D.; Koper, M. T. M. *Angew. Chemie Int. Ed.* 2020, *59* (2), 711–715.
- (23) Herasymenko, P.; Šlendyk, I. *Z Phys Chem A* 1930, No. 149, 123–139.
- (24) Frumkin, A. N. *Trans. Faraday Soc.* 1959, *55* (1), 156–167.
- (25) Waagele, M. M.; Gunathunge, C. M.; Li, J.; Li, X. *J. Chem. Phys.* 2019, *151* (16), 160902.